

A structure-based strategy to identify new molecular scaffolds targeting the bacterial ribosomal A-site

Nicolas Foloppe,* I-Jen Chen, Ben Davis, Adam Hold, Dave Morley and Rob Howes

Vernalis (R&D) Ltd, Granta Park, Abingdon, Cambridge CB1 6GB, UK

Received 14 October 2003; accepted 16 December 2003

Abstract—The need for novel antibiotics is widely recognized. A well validated target of antibiotics is the bacterial ribosome. Recent X-ray structures of the ribosome bound to antibiotics have shed new light on the binding sites of these antibiotics, providing fresh impetus for structure-based strategies aiming at identifying new ribosomal ligands. In that respect, the ribosomal decoding region of the aminoacyl-tRNA acceptor site (A-site) is of particular interest because oligonucleotide model systems of this site are available for crystallography, NMR and compound binding assays. This work presents how these different resources can be combined in a hierarchical screening strategy which has led to the identification of new A-site ligands. The approach exploits an X-ray structure of the A-site against which large and diverse libraries of compounds were computationally docked. The complementarity of the compounds to the A-site was assessed using a scoring function specifically calibrated for RNA targets. Starting from ≈ 1 million compounds, the computational selection of candidate ligands allowed us to focus the experimental work on 129 compounds, 34 of which showed affinity for the A-site in a FRET-based binding assay. NMR experiments confirmed binding to the A-site for some compounds. For the most potent compound in the FRET assay, a tentative binding mode is suggested, which is compatible with the NMR data and the limited SAR in this series. Overall, the results validate the screening strategy.

© 2004 Elsevier Ltd. All rights reserved.

1. Introduction

The global emergence of bacterial resistance to antibiotics is increasingly limiting the effectiveness of medically used antibacterial agents.^{1,2} Therefore, it is important to identify novel compounds which combine antibiotic activity with drug-like properties. The bacterial ribosome is one of the few well-validated molecular targets against which several classes of clinically relevant antibiotics are known to act.^{3,4} These classes include aminoglycosides, chloramphenicol, lincosamides, macrolides, oxazolidinones, streptogramins and tetracyclines. The structures of some of these antibiotics bound to the small (30S) or the large (50S) bacterial ribosomal subunits were recently obtained by X-ray crystallography.^{5–8} The functional relevance of these structures has been validated by their ability to rationalise a large body of genetic and biochemical data.^{9–11}

This structural information also provided crucial new insights regarding the binding sites, binding modes and mechanisms of action for several of these antibiotics, in particular some aminoglycosides.

Footprinting studies^{12,13} have long suggested that aminoglycosides bind to the decoding region of the aminoacyl-tRNA acceptor site (A-site) of 16S ribosomal RNA (rRNA). This site is involved in codon-anticodon recognition, consistent with the aminoglycosides exerting their antibiotic properties via a decrease in translational fidelity.¹⁴ Aminoglycosides tend to bind to the prokaryotic A-site with dissociation constants in the low micromolar range.^{15–17} NMR structures of RNA oligonucleotides^{18–20} and crystal structures of a 30S subunit,⁶ obtained with aminoglycoside paromomycin, confirmed that this antibiotic binds in the ribosomal decoding region, to an internal loop in helix 44 of 16S rRNA. The binding mode of paromomycin to 30S is, by and large, consistent with that observed in a higher resolution (2.5 Å) crystal structure of an RNA construct designed to mimic the A-site.²¹ This A-site fragment model system, however, provided an even more detailed picture of the interaction of paromomycin with rRNA, emphasising the role of water-mediated contacts. This

Abbreviations: FRET, Fluorescence Resonance Energy Transfer; MW, Molecular Weight; NMR, Nuclear Magnetic Resonance; NRot, Number of Rotatable Bonds; SAR, Structure–Activity Relationship.

Keywords: A-site; Drug design; FRET assay; Ribosome.

* Corresponding author. Tel.: +44-1223-895-338; fax: +44-1223-895-556; e-mail: n.foloppe@vernalis.com

system has also been used to obtain the structure of the aminoglycosides tobramycin,²² geneticin,²³ and of synthetic aminoglycosides²⁴ bound to the A-site.

Comparison of the binding modes of these aminoglycosides showed that their common neamine core interacts similarly and tightly with the A-site internal loop, stabilising a bulged-out conformation for the universally conserved adenines 1492 and 1493 (Fig. 1, *Escherichia coli* sequence numbering is used throughout). Disruption of the conformational dynamics of these adenines by aminoglycosides is consistent with these adenines playing a key role for the discrimination between cognate and non-cognate tRNAs during translation,^{25,26} and aminoglycosides inducing miscoding during protein synthesis.¹⁴ Bulging out of A1492 and A1493 is therefore believed to be an important mechanism mediating the antibiotic properties of aminoglycosides. This conformation is presumably stabilised by stacking of the neamine ring I on G1491 and hydrogen bonds between neamine and A1408 (Fig. 1). G1491 and A1408 are highly conserved in bacteria, but are replaced by adenine and guanine, respectively, in human cytosolic ribosomes. Consistent with the structures, biochemical, mutation and phylogenetic data indicate that these sequence differences largely account for the selectivity of

aminoglycosides with respect to bacterial and human cytosolic ribosomes.^{27–29} Arguably, novel A-site ligands should maximise interactions with G1491 and A1408 to become clinically relevant antibiotics.

This wealth of information has set the stage for a structure-based approach to finding novel chemical entities binding to the bacterial A-site.^{30–32} An increasingly powerful approach to discover small molecules binding to a target site is to computationally dock these molecules into the 3-dimensional structure of this site.^{33,34} The overall orientation of the small molecule, as well as its intramolecular conformations, are explored, and the interactions between receptor and putative ligand scored for each configuration.³⁵ This allows ranking of libraries of existing compounds according to their calculated interaction scores, and to prioritise the compounds for experimental assays. This virtual screening strategy is well established against protein targets (see for example^{33,34,36–38}). Indeed, the commercially available docking engines were primarily developed and tested for protein-ligand complexes,^{39–44} and only a few docking experiments against RNA targets have been presented.^{45–48} The output of a computational docking experiment strongly depends on the validity of the scoring function used.³⁵ The largely empirical nature of these scoring functions necessitates the development of scores specifically calibrated for nucleic acid targets, while remaining robust at protein-RNA interfaces. Such a scoring function has been implemented in the docking software RiboDock,⁴⁹ which can operate in high-throughput mode.

We present here how a computational screen of >1 million compounds against a crystal structure of the bacterial A-site RNA allowed the selection of compounds which were then tested in a cascade of experimental assays. A number of the selected, lead-like, compounds were active in a FRET-based assay probing binding to the bacterial A-site. NMR data suggested that the binding mode of at least one of these compounds may be of particular interest for subsequent elaboration.

2. Results and discussion

Starting from an electronic catalogue of over 1 million commercially available compounds,⁵⁰ computational and experimental filters were applied in a hierarchical way (Fig. 2). Computational filters were applied first, since they are well adapted to handle large numbers of compounds in a time and cost-effective way. These filters were first applied to restrict the subsequent screen to lead-like compounds. Then, computational docking was used to short-list compounds that are structurally complementary to the A-site. This strategy allowed concentrating experimental efforts on a list of 129 compounds only, four orders of magnitude less than the initial number. Binding to the A-site was assayed using both a FRET-based assay and NMR. The compound numbering given in Table 1 and Scheme 1 is used throughout. These compounds were subjected to quality

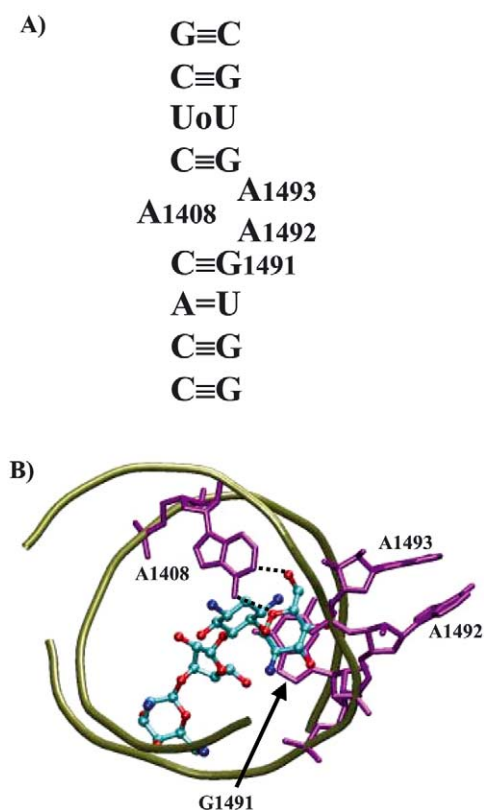


Figure 1. Overall view of the bacterial A-site. (A) Sequence of rRNA helix 44 in the vicinity of the *E. coli* A-site. Aminoglycosides target the internal loop, including G1491, A1492, A1493 and A1408 (*E. coli* sequence numbering). (B) Crystal structure of paromomycin bound to the A-site rRNA (Protein Data Bank entry 1J7T²¹). For clarity, only the RNA backbone trace is shown (tube), together with selected bases. Paromomycin binds in the RNA major groove, and ring I of paromomycin stacks on G1491 while hydrogen-bonding A1408. These hydrogen bonds are depicted with broken lines.

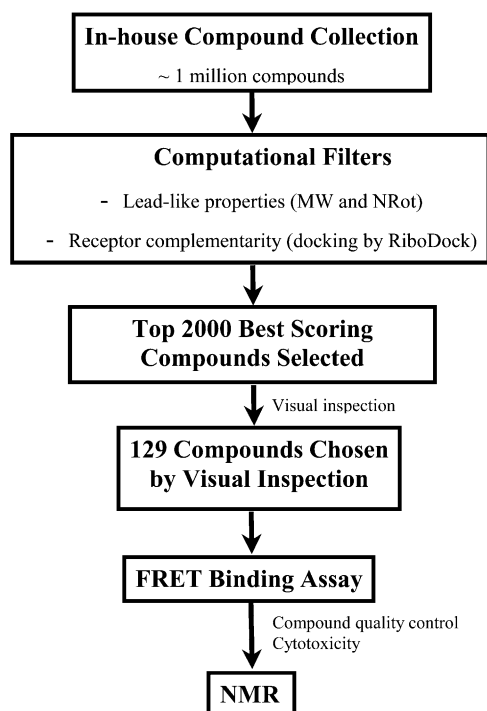
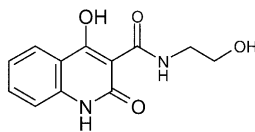


Figure 2. Flow-chart for the overall screening cascade.



Scheme 1. Compound 35.

control, the results of which were consistent with the structures shown.

Cytotoxicity was also tested on normal human cells (HEK293) using the Sulphorhodamine B assay, and only four compounds (**6**, **11**, **13**, **15**) were found to be cytotoxic according to the criteria given in Methods.

2.1. Computational screening

Both theoretical⁵¹ and empirical⁵² arguments suggest that lead compounds should be of relative limited complexity. In view of these arguments, computational filters were first applied to the in-house electronic libraries of compounds,⁵⁰ such that only compounds with less than seven rotatable bonds and molecular weight between 250 and 550 were kept for docking. Application of these filters is also expected to enrich the docking library with compounds having favourable absorption properties⁵³ and for which the conformational search during docking should be relatively efficient. This resulted in a set of $\approx 890\,000$ compounds which were docked into the bacterial A-site structure with the program RiboDock.

The volume accessible to each compound during docking (Fig. 3) was focused around the region of space occupied by the neamine moiety in the crystal structure of paromomycin bound to the target A-site structure,²¹

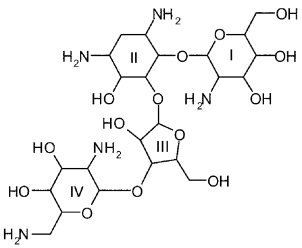
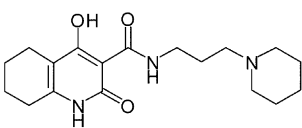
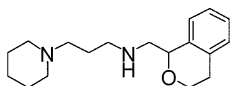
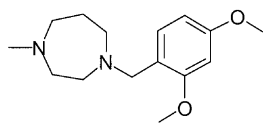
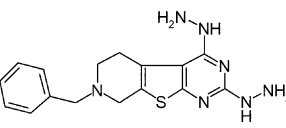
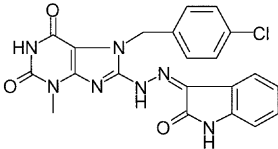
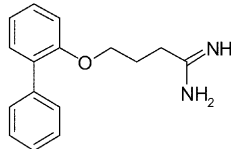
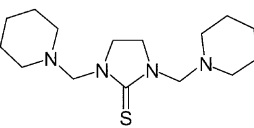
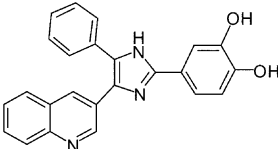
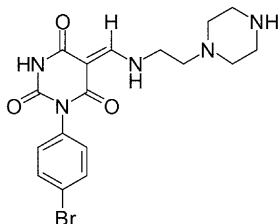
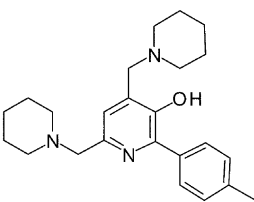
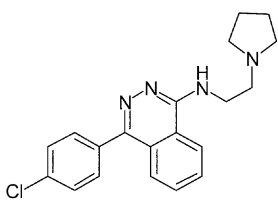
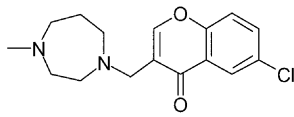
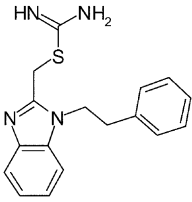
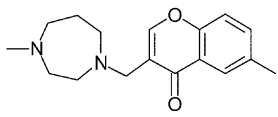
to bias the search towards ligands which would stack on G1491 and hydrogen-bond to A1408 (see Introduction for the importance of these interactions). The output of the docking was first filtered with a combination of RiboDock score components, to select compounds forming the most favourable interactions with the A-site while keeping internal strain low (see Methods). A balance between the polar and apolar contributions to the total score was kept, to remove compounds which are overly polar. Indeed, docking to RNA leads to total scores which can be dominated by the polar term, and can rank very favourably compounds which can form many hydrogen bonds with the phosphate backbone and the exposed edge of the bases. Using solely the total score, one may therefore select highly polar and charged scaffolds which are unlikely to be good lead candidates with respect to absorption and distribution properties. We therefore selected the 2000 best ranked compounds for which the apolar term reached a minimal threshold (see Methods).

For the sake of computational speed, empirical scoring functions like that used in RiboDock do not take long-range electrostatic (Coulombic) interactions explicitly into account. Yet, it is well documented that RNA ligands tend to be positively charged, as required for electrostatic complementarity to RNA.^{54–56} It was therefore interesting to check the overall net charge of the selected 2000 compounds. As shown in Table 2, the vast majority of these compounds had a net charge of +1 or +2. This shows that, although Coulombic interactions are not explicitly included in the RiboDock scoring function, it is well balanced to identify compounds with a meaningful overall net charge when targeting nucleic acids. For the selected 2000 compounds, this charge remained in a range compatible with drug-likeness.

The docking mode for each of these 2000 compounds was then inspected visually, to short-list molecules with a ring stacking on G1491 while hydrogen bonding to A1408 whenever possible. The output of this manual filtering was a list of 129 compounds to be tested in the FRET assay (see below).

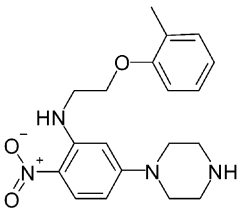
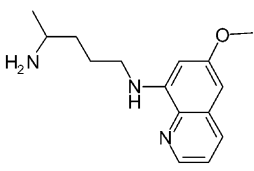
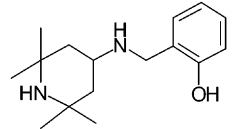
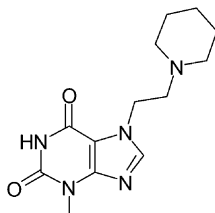
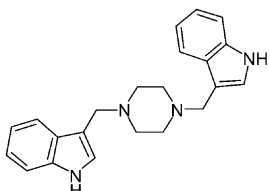
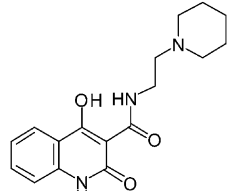
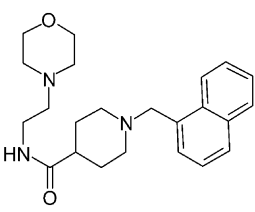
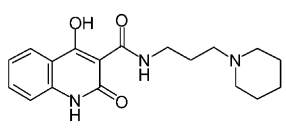
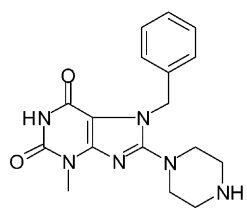
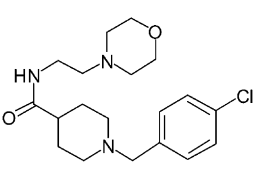
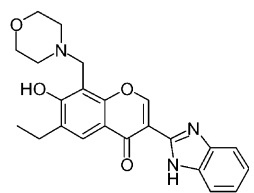
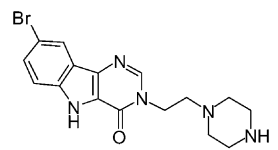
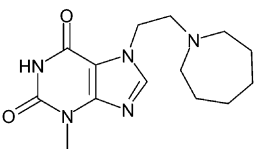
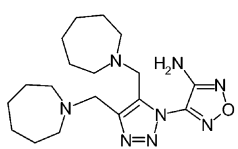
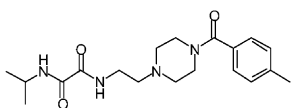
Examples of selected docking modes are given in Figure 4, for compounds which were active in the FRET assay. Although these docking modes are largely theoretical constructs in need of experimental testing, their visualisation is interesting because it shows that small organic molecules already exist, which have a good degree of complementarity to the bacterial A-site. For instance, the bicyclic system of compound **1** stacks on G1491, and its lactam moiety offers a two-pronged hydrogen-bonding complement to the edge of A1408. Branching off its ring system, the aliphatic chain of **1** follows the major groove curvature and positions a positively charged amine in a salt-bridge with a phosphate group. This docking mode for **1** is, to a large extent, compatible with the corresponding intermolecular NMR NOE data (see below). This suggests that virtual screening using empirical scoring functions can identify sensible candidate compounds for assay against this important therapeutic target. These docking modes may serve as

Table 1. List of compounds active in the FRET assay

Structure			
ID	PAR	1	2
$K_{i,app}$	12.3	17	18
NMR	Yes and NOEs	Yes and NOEs	Yes and NOEs
Structure			
ID	3	4	5
$K_{i,app}$	31	35	50
NMR	Yes and NOEs	No	No
Structure			
ID	6	7	8
$K_{i,app}$	53	109	111
NMR	Yes	No	Yes
Structure			
ID	9	10	11
$K_{i,app}$	137	143	146
NMR	Yes and NOEs	Yes	No
Structure			
ID	12	13	14
$K_{i,app}$	156	175	184
NMR	No	No	No

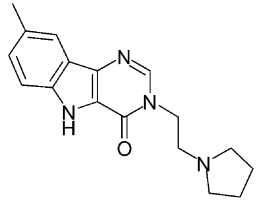
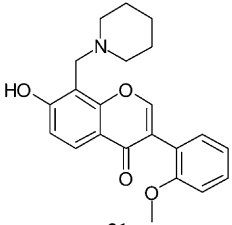
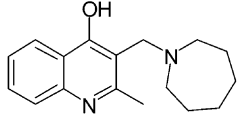
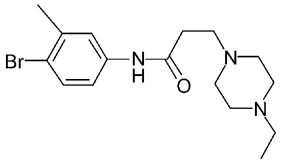
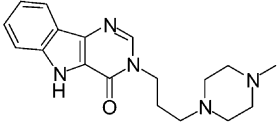
(continued on next page)

Table 1 (continued)

Structure			
ID	15	16	17
$K_{i,app}$	204	206	206
NMR	Yes	Yes	Yes
Structure			
ID	18	19	20
$K_{i,app}$	212	216	222
NMR	Yes	No	No
Structure			
ID	21	22	23
$K_{i,app}$	233	242	246
NMR	Yes and NOEs	No	No
Structure			
ID	24	25	26
$K_{i,app}$	250	251	264
NMR	No	No	Yes and NOEs
Structure			
ID	27	28	29
$K_{i,app}$	283	291	308
NMR	No	Yes	Yes

(continued on next page)

Table 1 (continued)

Structure			
ID	30	31	32
$K_{i,app}$	341	395	401
NMR	No	No	No
Structure			
ID	33	34	
$K_{i,app}$	419	426	
NMR	Yes and NOEs	No	

For every compound, are given its two-dimensional structure, identifier (ID) and $K_{i,app}$ (see Methods for the definition of $K_{i,app}$). NMR refers to whether the compound was tested in NMR ('Yes') or not ('No'), and mentions when intermolecular NOEs between the RNA and compound were observed ('Yes and NOEs').

working hypotheses for further elaboration of the corresponding compounds by medicinal chemistry.

2.2. FRET assay

The primary assay for screening the 129 compounds selected after the virtual screening was an A-site binding assay, based on Fluorescence Resonance Energy Transfer (FRET). This assay detects displacement of a fluorescent paromomycin derivative (TAMRA-paromomycin) from an oligonucleotide model of the ribosomal A-site (Fig. 5), by compounds which compete for binding to the A-site. When bound to the RNA, FRET takes place between the fluorescence donor TAMRA-paromomycin and the fluorescence acceptor dabcy group linked to the RNA. The assay monitors the fluorescence of the TAMRA group, which increases when TAMRA-paromomycin is displaced by another ligand. This assay has been extensively validated using a range of unlabelled aminoglycoside antibiotics.¹⁶ It is possible, however, that the conformations of the oligonucleotide used

to model the A-site may not reflect exactly those present in its 30S counterpart, which is a potential limitation of this assay.

Because the selected compounds were lead-like, and therefore comparatively small and simple, it was expected that some of them would be very weak binders. It is still of interest to detect these compounds because, if they are small enough, they can be subsequently improved with medicinal chemistry elaboration. Therefore each compound was initially tested in the FRET assay at the relatively high concentration of 500 μ M. This concentration was also selected keeping in mind that aminoglycoside antibiotics bind to the A-site with a moderate affinity only, in the low micromolar range.¹⁵ Active compounds were then assayed in a second step, a titration, which enabled ranking of every hit in the FRET assay according to an apparent K_i ($K_{i,app}$).

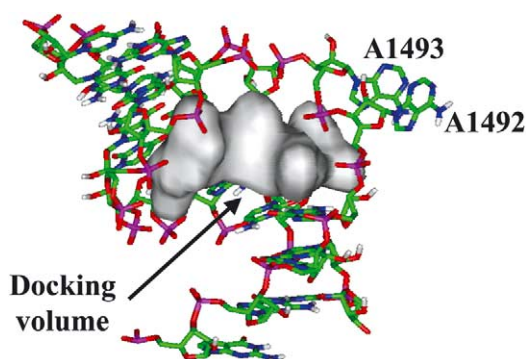


Figure 3. Volume accessible to the compounds during docking into the bacterial A-site. The RNA is viewed from the major groove.

Table 2. Net charge analysis for selected sets of compounds

Formal charge ^a	Top2000 ^b	FRET inactive ^c	FRET active ^d
-1	1 (<0.1%)	0 (0.0%)	0 (0.0%)
0	102 (5.1%)	24 (25.3%)	1 (2.9%)
1	812 (40.6%)	47 (49.5%)	17 (50.0%)
2	980 (49.0%)	23 (24.2%)	16 (47.1%)
3	89 (4.5%)	1 (1.1%)	0 (0.0%)
4	15 (0.8%)	0 (0.0%)	0 (0.0%)
5	0 (0.0%)	0 (0.0%)	0 (0.0%)
6	1 (<0.1%)	0 (0.0%)	0 (0.0%)
Total compounds ^e	2000	95	34
Average formal charge ^f	1.55	1.01	1.44

^a Net charge per compound. Every associated row gives the number of compounds having this charge in a given set of compounds.

^b Set of 2000 compounds selected for visual inspection after docking.

^c Set of compounds inactive in the FRET assay.

^d Set of compounds active in the FRET assay.

^e Total number of compounds in a given set.

^f Average net charges per compound in a given set.

Examples of such titration curves are shown in Figure 6. The 34 compounds which were active in the FRET assay are listed in Table 1.

On average, these compounds tend to carry a slightly higher net positive charge than those which are FRET-inactive (Table 2), consistent with binding to RNA. This average difference is, however, small (<half a charge), suggesting that activity in the FRET assay does not reflect only electrostatically driven non-specific RNA binding. This is also consistent with the range of observed $K_{i,app}$ values which varies 25 fold from the most potent (**1**, $K_{i,app}$ = 17 μ M) to the least potent (**34**, $K_{i,app}$ = 426 μ M) compound. For comparison, paromomycin has a $K_{i,app}$ of 12.3 μ M. It is interesting to note that even some comparatively small compounds, such as **3**, showed activity in the FRET assay, suggesting that A-site ligands do not need to be large poly-cationic molecules like aminoglycosides. Such simple scaffolds should be amenable to medicinal chemistry efforts.

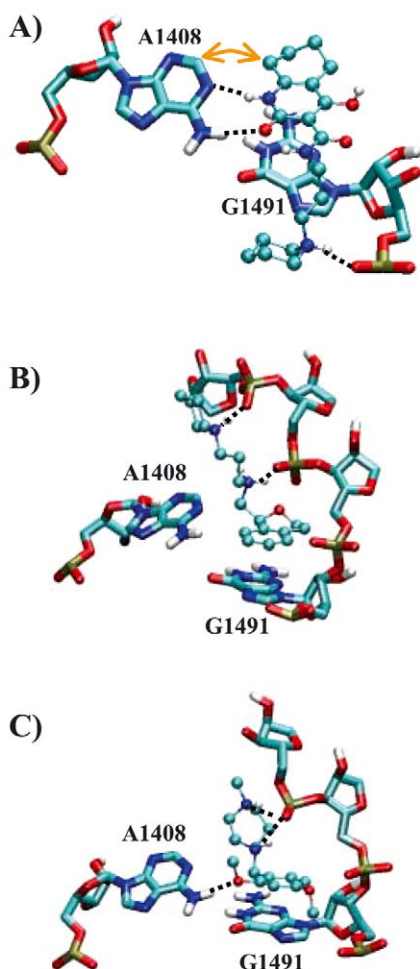


Figure 4. Examples of docking modes obtained from the virtual screening, for the three most active compounds in the FRET assay. Panels A, B and C correspond respectively to compounds **1**, **2** and **3** (see Table 1). The compounds are depicted in ball and line. Only part of the RNA, in the vicinity of the compounds, is shown. The RNA is depicted with sticks, and bases A1408 and G1491 are labelled. Hydrogen bonds are depicted with black broken lines. The orange curved arrow in panel A depicts an observed intermolecular NOE between H2 of A1408 and the aliphatic part of the bicyclic moiety of compound **1**.

Although the FRET active compounds are not large poly-cationic molecules, they frequently contain positively charged moieties like piperidine or piperazine, which are likely to interact favourably with the RNA backbone (Fig. 4). This is illustrated by the congeneric series of compounds **1**, **20**, **22** and **35**, where only the inactive compound (**35**, see Scheme 1) does not contain such a basic moiety. The replacement of the piperidine group in **20** ($K_{i,app}$ = 222 μ M) by a hydroxyl group in **35** is the only difference between these two compounds, and leads to a loss of activity. Activity in this series is not, however, just driven by electrostatic interactions, given that a partial reduction of the fused bicyclic system in **1** leads to a \approx 10-fold increase in potency as compared to that of **22**. This is compatible with the binding model in Figure 4A, where this bicyclic system interacts directly with the RNA bulge including A1408 and G1491. Interestingly, the aminoglycoside antibiotics bind to this bulge with an aliphatic, and not aromatic, ring. Indeed, inspection of the structures suggests that the slightly bulkier aliphatic rings fit more snugly in this RNA bulge. That the bicyclic system of compound **1** binds to this bulge is also supported by the NMR data.

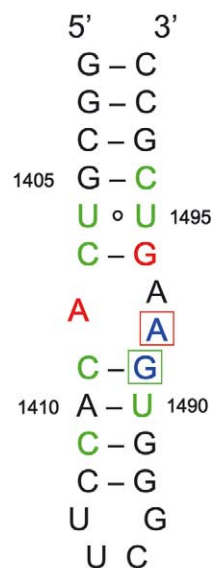


Figure 5. RNA oligonucleotide used to model the A-site in the FRET assay and NMR experiments. When used in the FRET assay, a fluorescence acceptor dabcy group was linked to the 3'-terminus of the oligonucleotide. Compound **1** is also shown to summarize some of the NMR results obtained with the RNA:compound **1** complex. Resonances involved in intermolecular NOEs in this complex are indicated in red and blue on both compound **1** and the RNA. Nucleotides for which significant chemical shift changes are observed in either the TOCSY or 1D imino spectra upon binding of the ligand are indicated in green. Residues which give rise to NOEs to both regions of compound **1** are boxed. G1491 has both intermolecular NOEs to compound **1** and significant chemical shift changes in the 1D imino spectrum. A1492 showed intermolecular NOEs to both the aliphatic ring and the side-chain of compound **1**.

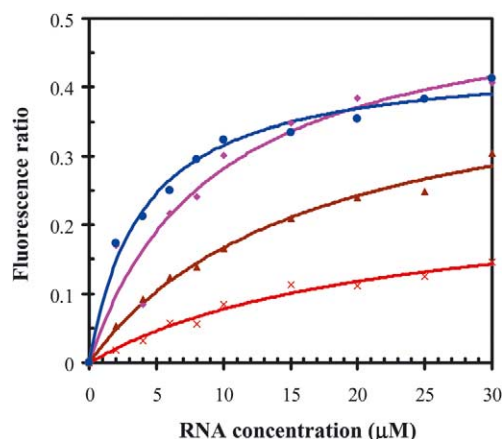


Figure 6. Typical titration curves obtained in the FRET-based assay. These curves were obtained in presence of compound **1** (×), compound **3** (▲), and of an inactive compound (●). These curves were obtained at a concentration of 125 μM for the active compounds **1** and **3**, and a concentration of 500 μM for the inactive compound. The control without compound is also shown (◆). The fluorescence ratio is defined as $1 - (\text{Fluorescence intensity of TAMRA-paromomycin with compound, at a given RNA concentration} / \text{Fluorescence intensity of TAMRA-paromomycin with compound, without RNA})$.

2.3. NMR

For 16 of the compounds active in the FRET assay, 2D NMR was used to further ascertain binding of these compounds to the RNA. The criteria used to select the compounds tested in these experiments included their solubility and availability in suitable amounts. For these compounds, NOESY spectra were obtained in presence of an A-site RNA oligonucleotide (Fig. 5). The results of these NOESY experiments are summarised in Table 1. Of course, an absence of intermolecular NOEs does not mean absence of binding. Seven compounds, including the three most active in the FRET assay, showed unambiguous intermolecular NOEs with the A-site RNA, confirming binding of these compounds to the RNA.

In particular, compound **1** gave good quality, well resolved, intermolecular NOE data (Fig. 7). Spectra of the A-site RNA:compound **1** complex were analysed in more detail than those obtained for other compounds. Intermolecular NOEs were assigned based on comparison of the TOCSY and NOESY spectra with previously determined assignments for the A-site RNA in the free

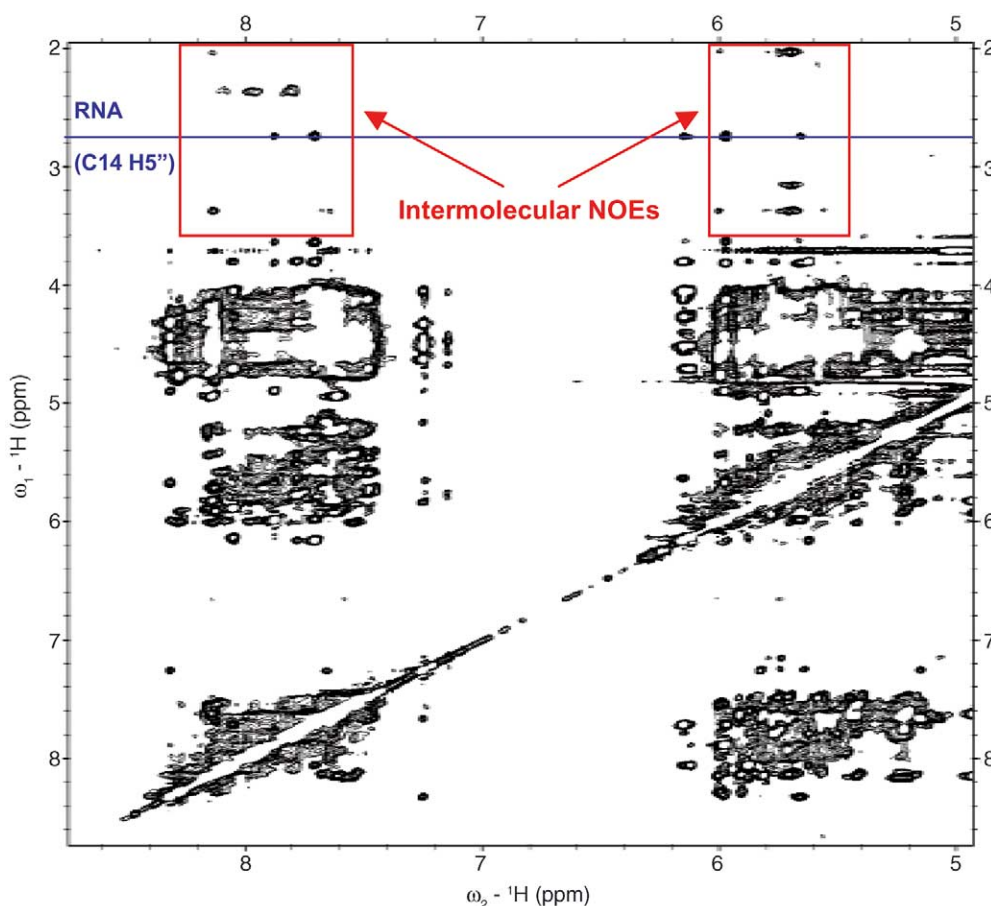


Figure 7. The aromatic fingerprint region of a 400 ms NOESY of the A-site RNA: compound **1** complex recorded in 100% D_2O at 298 K. The concentration of both components in the complex was ~ 1.0 mM. Compound **1** does not contain observable resonances at chemical shifts greater than 5 ppm, whilst the A-site RNA contains only one resonance below 3.6 ppm ($\text{C14H5}'$, indicated by a blue line). The red boxed regions therefore exclusively contain intermolecular NOEs (except for those at the frequency of $\text{C14H5}'$).

and paromomycin bound states (D. Fourmy, personal communication). A tentative assignment of the observed intermolecular NOEs was made (Fig. 5). These NOEs were to the internal loop region of the A-site. This region is flanked by areas of the RNA where pyrimidine chemical shifts changes were observed upon binding of the ligand (Fig. 5). The observed NOEs and chemical shift changes suggest a binding mode with the bicyclic ring system contacting the bases forming the internal loop, with the charged sidechain orientated towards the phosphate groups. In particular, an intermolecular NOE is observed between H2 of A1408 and the aliphatic part of the bicyclic ring of compound **1**, which are within 4.0 Å of each other in the binding mode shown in Figure 4. This is consistent with the elements of structure–activity relationship presented above for the associated series of compounds.

The docking model of compound **1** shown in Figure 4 is compatible with the NMR data and the available SAR, although further data would be needed to propose a structural model with greater confidence. Multiple binding modes for compound **1** are possible, especially because this compound would still hydrogen-bond A1408 if the docking mode shown in Figure 4 was flipped around the long axis of the bicyclic system. Incidentally, this may entropically favour binding to the A-site. Both docking modes bring the bicyclic system of compound **1** in the vicinity of residues A1492 and A1493. This is potentially of great interest, as there is good evidence that it is this type of interaction which mediates the antibiotic mechanism of action of the aminoglycosides.^{6,25}

3. Conclusions

This work presented how the recently determined crystal structures of the bacterial ribosomal A-site can be exploited for structure-based virtual screening (docking), leading to the discovery of new ligands for this site of great therapeutic interest. The high-throughput docking software suite, RiboDock, allowed rapid screening of ~1 million commercially available, chemically diverse compounds, allowing prioritisation of a far smaller number (129) of compounds for experimental assays. Binding of these compounds to an A-site RNA oligonucleotide was first tested using a FRET-based assay developed in-house, showing that about a quarter of the compounds were active in this assay. These compounds passed simple tests for quality control, and only four compounds showed signs of cytotoxicity at 25 µM with eukaryotic cell cultures. The relative affinities of these active compounds for the A-site oligonucleotide RNA were ranked using titrations. Analysis of the results indicates that, on average, non-specific electrostatic interactions are not sufficient for compounds to be active in this FRET assay. This further validates this type of assay for screening purposes. For selected compounds, the detection of intermolecular NOEs by NMR, between compound and A-site RNA oligonucleotide, confirmed binding of these compounds to the RNA.

These results highlighted a chemical series of particular interest, represented by compound **1**, the most potent in the FRET assay. The intermolecular NOEs are consistent with compound **1** binding to the targeted RNA bulge of the A-site, with a cyclic moiety stacking on G1491 and contacting A1408, A1492 and A1493. This corresponds to an overall binding mode consistent with the limited SAR in this series. These observations, combined with computational models, suggest that compound **1** hydrogen-bonds A1408. Therefore, there is preliminary evidence that this compound forms some of the contacts which are key to the selectivity of A-site binding antibiotics for prokaryotes, and to their mechanism of action. In addition, compounds in this series were not found to be particularly toxic to eukaryotic cells, and are arguably amenable to elaboration by medicinal chemistry. Taken altogether, these results suggest that it is worth exploiting this series further.

4. Computational and experimental methods

4.1. Computational screening

The crystal structure of an A-site rRNA construct bound to paromomycin (Protein Data Bank⁵⁷ entry 1J7T²¹) was selected to prepare the target site for docking, using the most ordered of the two A-sites contained in this construct. Paromomycin and water molecules were removed from the coordinates, and polar hydrogens added to RNA using the CHARMM force-field.⁵⁸

The preparation of the screened electronic catalogue of commercially available compounds, as well as details of the docking engine RiboDock, have been presented elsewhere,^{49,50} and only specific points relevant to the present work are re-iterated here. Filtering of the catalogue of compounds on molecular weight ($250 < MW < 550$) and number of rotatable bonds ($NRot < 7$) to prepare the set of compounds used for docking was performed with in-house perl scripts. The initial 3-dimensional structure of these compounds was then generated with CORINA,⁵⁹ with removal of counterions or solvent fragments, all chemical functionalities in their neutral state, and generation of multiple ring conformations within 7 kJ/mol of the lowest energy ring conformation. Only one stereoisomer per compound was generated, which is a limitation of this protocol because several stereoisomers exist for some compounds. Therefore some true ligands may be missed if the stereoisomer which binds was not docked.

Docking of these molecules was carried out with RiboDock on a PC cluster of 100 CPUs. Acidic functionalities were deprotonated, basic functionalities protonated, and apolar hydrogens removed with RiboDock. The Monte Carlo/simulated annealing protocol initially used in RiboDock⁴⁹ was replaced by a steady state Genetic Algorithm (GA) to improve the efficiency of the docking search. Ligand docking poses were represented using a conventional chromosome representation of translation, rotation, and rotatable bond dihedral

angles. A single GA population was used, of size proportional to the number of ligand rotatable bonds, with a mutation:crossover ratio of 3:2. The overall orientation and internal conformation of the compounds were searched with the GA, while the A-site receptor was kept fixed. This conformational search was performed in conjunction with an empirical scoring function specifically calibrated to reproduce the experimental binding mode of RNA ligands in known structures of complexes, and on the ability to discriminate between native and non-native ligands.⁴⁹ The RiboDock scores can be reported on an energy scale in kJ/mol, although the size of the RNA-ligand training set prevented a rigorous statistical fit to binding free energies.⁴⁹ This type of scoring function is made of a sum of chemically intuitive energy terms.³⁵ The RiboDock total score is the sum of intramolecular and intermolecular contributions. The intermolecular part can be further dissected in polar (e.g., hydrogen bond) and apolar (e.g., hydrophobic contacts) interactions. Only compounds which reached a total score of -20.0 kJ/mol or better were saved for further analysis. From this set, were kept only compounds with (i) an intramolecular score ≤ 5.0 kJ/mol (ii) an intermolecular polar score ≤ -12.5 kJ/mol and (iii) an intermolecular apolar score ≤ -12.5 kJ/mol. These filters aimed to remove strained conformations and to keep a balance between polar and apolar interactions formed between the receptor and putative ligands. The docking modes which passed these filters were then ranked according to their total intermolecular score, and the docking modes of the 2000 best-scoring compounds were inspected visually. Visual inspection allowed the discarding of docking modes unlikely to lead to real binding, for instance when large voids were present between ligand and RNA, or when the ligands projected large hydrophobic moieties into the solvent.

For the analysis of the net formal charge of the compounds active in the FRET assay, this charge was calculated with MOE,⁶⁰ assuming a pH of 7.0 and standard pK_a s in aqueous solution for the titratable groups.

Pictures of three-dimensional molecular structures were prepared with VMD,⁶¹ using the CPK colour code for hydrogen (white), carbon (green), nitrogen (blue) and oxygen (red) for compounds.

4.2. FRET assay

Binding to the A-site was tested for the selected 129 compounds with a Fluorescence Resonance Energy Transfer (FRET) assay. This assay exploits a known A-site ligand, a derivative of paromomycin tagged with the fluorescent FRET donor tetramethylrhodamine (TAMRA), as previously described.¹⁶ TAMRA-paromomycin inhibits an *in vitro* *E. coli* translation system with an IC_{50} of $0.4 \mu\text{M}$.¹⁶ TAMRA-paromomycin also binds to an oligoribonucleotide that models the bacterial ribosomal A-site, with the sequence shown in Figure 5. This oligonucleotide incorporates a 3'-dabcyl group as a non-fluorescent FRET acceptor (obtained from Xeragon Oligoribonucleotides, USA). Upon binding of

TAMRA-paromomycin to the RNA, FRET takes place between the TAMRA and dabcyl dyes, such that a reduction in donor fluorescence is observed.¹⁶ A compound competing with TAMRA-paromomycin for binding to the A-site leads to a reduction in the FRET activity between the TAMRA and dabcyl groups. Therefore, increase of the fluorescence intensity of the TAMRA group was used to detect the competitive binding of another compound to the A-site. This assay has been validated with a series of unlabelled aminoglycoside antibiotics which compete for binding and have K_i values in the micromolar range,¹⁶ using the same protocol as detailed below. TAMRA-paromomycin binds the oligonucleotide with a 15 nM affinity.¹⁶

Testing of the 129 compounds was performed in 96-well plates (costar 3915) at room temperature, in two steps. First, binding to the A-site oligonucleotide was detected at a single concentration of compound. Second, the RNA was titrated to ascertain true binding, as opposed to possible false positive results in single point measurements. The format for the assay was similar during these two steps.

During the first step, a fixed concentration of compound ($500 \mu\text{M}$) was added to a solution of 10 nM TAMRA-paromomycin in the presence of 100 mM Tris-HCl pH7.5, 50 mM KCl in a total volume of $100 \mu\text{L}$. Each compound was tested in duplicate. This was incubated for 60 min to reach equilibrium with respect to the interaction of TAMRA-paromomycin with the 96-well plate. A fixed amount of A-site oligonucleotide (30 nM) was added to the assay mixture and incubated for another 60 min to reach equilibrium. The FRET activity was measured on a Wallac Victor fluorimeter (excitation $544 \text{ nm}/10$, emission $590 \text{ nm}/10$) and determined as the ratio of the fluorescence emission of TAMRA-paromomycin in the absence of RNA to the emission in the presence of RNA. At this concentration of oligonucleotide there is a fixed decrease in donor fluorescence, due to FRET taking place. This decrease in donor fluorescence in absence of compound was compared to its counterpart in presence of compound. Compounds associated with a decrease in FRET activity were presumed to compete with TAMRA-paromomycin for binding to the A-site RNA.

In a second step, these compounds were tested in a titration with a fixed concentration of compound ($500 \mu\text{M}$), but varying amounts of A-site RNA. The active compounds (K_{app}/K_d greater than control) were then titrated again at a compound concentration of $125 \mu\text{M}$, to obtain a more accurate determination of $K_{i,\text{app}}$ values (Table 1, Fig. 6). These titrations were performed by varying the RNA concentration, rather than that of the compound, because this uses smaller amounts of RNA. The protocol for this format of the assay was identical to the single point assay, except that after the first incubation, varying amounts of A-site RNA were added to each well resulting in a titration from 0 to 30 nM of RNA. Each data set was fitted using the Michaelis-Menten steady state model to obtain the $K_{d,\text{app}}$. The K_d of TAMRA-paromomycin ($K_{d,\text{TAMRA}}$) to the A-site

oligonucleotide was calculated to be 15 nM. The apparent K_i ($K_{i,app}$) for each compound was calculated using the formula:

$$K_{i,app} = (1/(K_{d,app}/K_{d,TAMRA}) \times [\text{compound}])$$

This value of $K_{i,app}$ was used to rank compounds according to their affinity for the A-site RNA (Table 1).

4.3. Compound quality control

Every compound active in the FRET assay was subjected to a liquid chromatography-mass spectrometry (LC-MS) analysis, and the chemical structures given in Table 1 were consistent with the masses obtained by MS, to a purity of at least 85%. Purity was assessed by UV detection at three wavelengths and total ion current under positive ion electrospray. Details were as follows.

4.3.1. Materials. AnalaR grade Formic Acid (98/100%) was from BDH laboratory supplies (Poole, UK). HPLC grade Acetonitrile was purchased from Romil (Cambridge, UK). Purified water was produced using a Milli-Q gradient water system from Millipore (Watford, UK). HPLC grade Ammonium Acetate was obtained from Fisher Scientific (Loughborough, UK). AnalaR grade Dimethyl Sulphoxide DMSO was from BDH laboratory supplies (Poole, UK).

4.3.2. Preparation of samples. The analytes were dissolved in DMSO to a concentration of 20 mM, and these stock solutions were diluted 1 μ L of stock with 19 μ L of DMSO. The injection volume was 5 μ L.

4.3.3. Instrumentation: LC-MS analysis. Chromatographic separations were performed using an 1100 Series liquid chromatograph (Agilent Technologies, Palo Alto, CA, USA) consisting of a binary pump, mobile phase degasser, autosampler, UV-vis detector. Mobile phase A contained water with 10 mM Ammonium Acetate, 0.08% formic acid and mobile phase B contained 95% acetonitrile, 5% mobile phase A, 0.08% formic acid. The eluent flow after the UV-Vis detector was split 1:4 before entering an MSD 1100 (Agilent Technologies) single quadrupole mass spectrometer equipped with an electrospray (ESI) ionisation source.

Reverse phase chromatography was used, with a 3.6 \times 30 mm, 3- μ M particle C18(2) Luna column (Phenomenex, Macclesfield, UK) protected with a 4 mm C18 Security Guard (Phenomenex, Macclesfield, UK) guard cartridge. Detection was at 210 nm, 254 nm and 270 nm and positive ion ESI scanning a molecular weight range of 150–1000 AMU.

A gradient was used as follows: 0 \rightarrow 0.25 min, 5% B, 2 mL min⁻¹; 0.25 \rightarrow 2.5 min, 95% B, 2 mL min⁻¹; 2.5 \rightarrow 2.55 min, 95% B, 3 mL min⁻¹; 2.55 \rightarrow 3.6 min, 95% B, 3 mL min⁻¹; 3.6 \rightarrow 3.65 min, 95% B, 2 mL min⁻¹; 3.65 \rightarrow 3.7 min, 5% B, 2 mL min⁻¹; 3.7 \rightarrow 3.75 min, 5% B, 2 mL min⁻¹.

4.4. NMR

4.4.1. Preparation of RNA samples. A 27 nucleotide RNA molecule (Fig. 5) corresponding to the A-site of the *E. coli* 30S ribosomal subunit was prepared by in vitro transcription from an oligonucleotide template (Fourmy et al., 1996). The RNA sequence used was:



The RNA was purified by polyacrylamide gel electrophoresis, electroeluted from gel slices, dialyzed exhaustively against 1M NaCl, desalted and dialyzed against water. Samples were dried under vacuum and resuspended in the NMR buffer (20 mM potassium phosphate, pH 6.2, 0.2 mM EDTA, 100% D₂O or 90% H₂O/10% D₂O).

4.4.2. Spectroscopy. NMR spectra were recorded on a Bruker DRX600 spectrometer at 298 K. Samples contained approximately 1 mM RNA and compound to be tested. Spectra for all samples were acquired under automation using ICONNMR as part of the NMR screening process.

Spectra were acquired under automation using pre-saturation for solvent suppression. Standard TOCSY and NOESY spectra were recorded as described elsewhere.⁶² Spectra were processed manually using XWINNMR. A first order polynomial baseline correction was applied to all spectra in both the direct and indirect dimensions. 1D spectra of RNA:compound 1 complex in 90% H₂O/10% D₂O were acquired using watergate water suppression.⁶³

NOESY spectra of each RNA:compound complex were analysed for the presence of intermolecular NOES. Since all compounds studied contained resonances distinct from RNA resonances (1.0–3.5 ppm, 6.0–7.0 ppm), this analysis was rapid.

4.5. Cytotoxicity assay

HEK293 cells were grown under standard conditions in DMEM/10% foetal bovine serum (FBS)/1000 units/mL Pen/Strep. To assay cytotoxicity, 3600 cells were added to each well of a 96-well plate (Nunc #167008) and allowed to attach overnight. Next day, compounds were serially diluted in DMEM/10% FBS/Pen Strep/2% DMSO and then added to the HEK293 cells in the 96 well plate. The highest final concentration of the compounds was 80 μ M. The cells were incubated for 72 h in the presence of the compound. After this time the cells were washed once in phosphate buffered saline (PBS) and fixed for 30 min on ice in 10% Trichloroacetic acid. The plates were washed 3 times in water and dried in the incubator. To each well 100 μ L 0.4% Sulphorhodamine B (SRB) in 1% acetic acid was added and incubated for 15 min at room temperature. After this the plate was washed 3 times in 1% acetic acid. The plate was dried and the SRB solubilised using 100 μ L 10 mM Tris base. To calculate the GI₅₀, the A₅₄₀ was measured using a Wallac Victor. From these data, the GI₅₀ was calculated

using a general sigmoidal curve with Hill slope (a to d model). A compound was deemed to be cytotoxic if it had a GI₅₀ of <25 μ M.

Acknowledgements

We thank Drs. F. Aboul-ela, M. Afshar, H. Finch, B. Garmendia-Doval, G. Lentzen, N. Matassova, A. Murchie, C. Richardson and T. Sweeney for helpful discussions. We also thank Pr. E. Westhof for helpful discussions.

References and notes

- Walsh, C. *Nature* **2000**, 406, 775.
- Coates, A.; Hu, Y.; Bax, R.; Page, C. *Nature Reviews Drug Discovery* **2002**, 1, 895.
- Cundliffe, E.; Gale, E. F.; Cundliffe, E.; Reynolds, P. E.; Richmond, M. H.; Waring, M. J. *The Molecular Basis of Antibiotic Action*; John Wiley and Sons: New York, 1981; pp. 402–457.
- Vazquez, D. *FEBS Lett.* **1974**, 40, 63.
- Brodersen, D. E.; Clemons, W. M., Jr.; Carter, A. P.; Morgan-Warren, R. J.; Wimberly, B. T.; Ramakrishnan, V. *Cell* **2000**, 103, 1143.
- Carter, A. P.; Clemons, W. M.; Brodersen, D.; Morgan-Warren, R. J.; Wimberly, B. T.; Ramakrishnan, V. *Nature* **2000**, 407, 340.
- Pioletti, M.; Schlünzen, F.; Harms, J.; Zavirach, R.; Glühmann, M.; Avila, H.; Bashan, A.; Bartels, H.; Auebach, T.; Yonath, A.; Franceschi, F. *EMBO J.* **2001**, 20, 1829.
- Schlünzen, F.; Zarivach, R.; Harms, J.; Bashan, A.; Tocilj, A.; Albrecht, R.; Yonath, A. *Nature* **2001**, 413, 814.
- Ramakrishnan, V. *Cell* **2002**, 108, 557.
- Moore, P. B. *Biochemistry* **2001**, 40, 3243.
- Hansen, J. L.; Ippolito, J. A.; Ban, N.; Nissen, P.; Moore, P. B.; Steitz, T. A. *Molecular Cell* **2002**, 10, 117.
- Moazed, D.; Noller, H. F. *Nature* **1987**, 327, 389.
- Woodcock, J.; Moazed, D.; Cannon, M.; Davies, J.; Noller, H. F. *EMBO Journal* **1991**, 10, 3099.
- Davies, J.; Gorini, L.; Davis, B. *Mol. Pharmacol.* **1965**, 1, 93.
- Ryu, D. H.; Rando, R. R. *Bioorganic Medicinal Chemistry* **2001**, 9, 2601.
- Knowles, D. J. C.; Karn, J.; Murchie, A. I. H.; Lentzen, G. F. *PCT Int. Appl. WO 01/44505* **2001**.
- Wang, Y.; Hamasaki, K.; Rando, R. R. *Biochemistry* **1997**, 36, 768.
- Fourmy, D.; Recht, M. I.; Blanchard, S. C.; Puglisi, J. D. *Science* **1996**, 274, 1367.
- Fourmy, D.; Recht, M. I.; Puglisi, J. D. *J. Mol. Biol.* **1998**, 277, 347.
- Lynch, S. R.; Gonzalez, R. L., Jr.; Puglisi, J. D. *Structure* **2003**, 11, 43.
- Vincens, Q.; Westhof, E. *Structure* **2001**, 9, 647.
- Vincens, Q.; Westhof, E. *Chem. Biol.* **2002**, 9, 747.
- Vincens, Q.; Westhof, E. *J. Mol. Biol.* **2003**, 326, 175.
- Russell, R. J. M.; Murray, J. B.; Lentzen, G.; Haddad, J.; Mobashery, S. *J. Am. Chem. Soc.* **2003**, 125, 3410.
- Ogle, J. M.; Brodersen, D. E.; Clemons, W. M., Jr.; Tarry, M. J.; Carter, A. P.; Ramakrishnan, V. *Science* **2001**, 292, 897.
- Ogle, J. M.; Murphy, I. V. F. V.; Tarry, M. J.; Ramakrishnan, V. *Cell* **2002**, 111, 721.
- Böttger, E. C.; Springer, B.; Prammananan, T.; Kidan, Y.; Sander, P. *EMBO* **2001**, 2, 318.
- Recht, M. I.; Douthwaite, S.; Puglisi, J. D. *EMBO J.* **1999**, 18, 3133.
- Beauclerk, A. A. D.; Cundliffe, E. *J. Mol. Biol.* **1987**, 193, 661.
- Haddad, J.; Kotra, L. P.; Llano-Sotelo, B.; Kim, C.; Azucena, E. F.; Liu, M.; Vakulenko, S. B.; Chow, C. S.; Mobashery, S. *J. Am. Chem. Soc.* **2002**, 124.
- Knowles, D.; Foloppe, N.; Matassova, N. B.; Murchie, A. I. H. *Curr. Opin. in Pharmacology* **2002**, 2, 501.
- Vourloumis, D.; Takahashi, M.; Winters, G. C.; Simonson, K. B.; Ayida, B. K.; Barluenga, S.; Qamar, S.; Shandrick, S.; Zhao, Q.; Hermann, T. *Bioorg. Med. Chem. Lett.* **2002**, 12, 3367.
- Schneider, G.; Böhm, H. *J. Drug Discovery Today* **2002**, 7, 64.
- Abagayan, R.; Totrov, M. *Current Opinion in Chemical Biology* **2001**, 5, 375.
- Böhm, H. J.; Stahl, M. In *Reviews in Computational Chemistry, Vol. 18*; Lipkowitz, K. B., Boyd, D. B., Eds.; Wiley-VCH: New York, 2002; p 41–87.
- DesJarlais, R. L.; Seibel, G. L.; Kuntz, I. D.; Furth, P. S.; Alvarez, J. C.; Ortiz de Montellano, P. R.; DeCamp, D. L.; Babe, L. M.; Craik, C. S. *Proc. Natl. Acad. Sci. U.S.A.* **1990**, 87, 6644.
- Grüneberg, S.; Stubbs, M. T.; Klebe, G. *J. Med. Chem.* **2002**, 45, 3588.
- Schoichet, B. K.; Stroud, R. M.; Santi, D. V.; Kuntz, I. D.; Perry, K. M. *Science* **1993**, 259, 1445.
- Vieth, M.; Hirst, J. D.; Kolinski, A.; Brooks, C. L., III *J. Comp. Chem.* **1998**, 19, 1612.
- Bissantz, C.; Folkers, G.; Rognan, D. *J. Med. Chem.* **2000**, 43, 4759.
- Stahl, M.; Rarey, M. *J. Med. Chem.* **2001**, 4, 1035.
- Wei, B. Q.; Baase, W. A.; Weaver, L. H.; Matthews, B. W.; Shoichet, B. K. *J. Mol. Biol.* **2002**, 322, 339.
- Nissink, J. W. M.; Myrray, C.; Hartshorn, M.; Verdonk, M. L.; Cole, J. C.; Taylor, R. *Proteins* **2002**, 49, 457.
- Krammer, B.; Rarey, M.; Lengauer, T. *Proteins* **1999**, 37, 228.
- Leclerc, F.; Karplus, M. *Theor. Chem. Acc.* **1999**, 101, 131.
- Chen, Q.; Shafer, R. H.; Kuntz, I. D. *Biochemistry* **1997**, 36, 11402.
- Filikov, A. V.; Mohan, V.; Vickers, T. A.; Griffey, R. H.; Cook, P. D.; Abagayan, R. A.; James, T. L. *J. Comput. Aided Mol. Design* **2000**, 14, 593.
- Lind, K. E.; Du, Z.; Fujinaga, K.; Peterlin, B. M.; James, T. L. *Chemistry & Biology* **2002**, 9, 185.
- Morley, S. D.; Afshar, M. submitted to *J. Comput.-Aided Mol. Des.*
- Knowles, D. *Current Drug Discovery* **2002**, December, 31–35.
- Hann, M. M.; Leach, A. R.; Harper, G. *J. Chem. Inf. Comput. Sci.* **2001**, 41, 856.
- Oprea, T. I.; Davis, A. M.; Teague, S. J.; Leeson, P. D. *J. Chem. Inf. Comput. Sci.* **2001**, 41, 1308.
- Lipinski, C. A.; Lombardo, F.; Dominy, B. W.; Feeney, P. J. *Adv. Drug Deliv. Reviews* **1997**, 23, 3.
- Walter, F.; Vincens, Q.; Westhof, E. *Current Opinion in Chemical Biology* **1999**, 3, 694.
- Hermann, T. *Angew. Chem., Int. Ed.* **2000**, 39, 1890.
- Ma, C.; Baker, N. A.; Joseph, S.; McCammon, J. A. *J. Am. Chem. Soc.* **2002**, 124, 1438.
- Berman, H. M.; Westbrook, J.; Feng, Z.; Gilliland, G.; Bhat, T. N.; Weissig, H.; Shindyalov, I. N.; Bourne, P. E. *Nucleic Acids Research* **2000**, 28, 235.

58. Foloppe, N.; MacKerell, A. *J. Comp. Chem.* **2000**, *21*, 86.
59. Gasteiger, J.; Rudolph, C.; Sadowski, J. *Tetrahedron Computer Methodology* **1990**, *3*, 537.
60. <http://www.chemcomp.com>.
61. Humphrey, W.; Dalke, A.; Schulten, K. *J. Mol. Graph.* **1996**, *14*, 33.
62. Varani, G.; Aboul-ela, F.; Allain, F. H. T. *Progress in Nuclear Magnetic Resonance Spectroscopy* **1996**, *29*, 51.
63. Sklenar, V.; Piotto, M.; Leppik, R.; Saudek, V. *Journal of Magnetic Resonance, Series A* **1993**, *102*, 241.